OUKA
The University of Osaka
Institutional Knowledge Archive

Title	3-Azafluorenone Derivatives with Small HOMO-LUMO Gaps, Allowing Visible-Light Absorption
Author(s)	Kobayashi, Toshimichi; Itabashi, Yuki; Iwai, Kento et al.
Citation	Chemistry - An Asian Journal. 2025, p. e70415
Version Type	AM
URL	https://hdl.handle.net/11094/103024
rights	© 2025 Wiley-VCH GmbH
Note	

The University of Osaka Institutional Knowledge Archive : OUKA

https://ir.library.osaka-u.ac.jp/

The University of Osaka

RESEARCH ARTICLE

3-Azafluorenone Derivatives with Small HOMO–LUMO Gaps, Allowing Visible-Light Absorption

Toshimichi Kobayashi,[a] Yuki Itabashi,[b] Kento Iwai,[c] Tsuyoshi Inoue,[a, b] Kei Ohkubo,[b, d] and Haruyasu Asahara*[a, b]

[a] T. Kobayashi, T. Inoue, H. Asahara
Graduate School of Pharmaceutical Sciences
The University of Osaka
1-6 Yamada-oka, Suita, Osaka 565-0871, Japan
E-mail: asahara@phs.osaka-u.ac.jp

[b] Y. Itabashi, T. Inoue, K. Ohkubo, H, Asahara
Institute for Open and Transdisciplinary Research Initiatives (OTRI)
The University of Osaka
1–6 Yamada-oka, Suita, Osaka 565–0871, Japan

[c] K. Iwai
Department of Chemistry, Faculty of Science
Nara Women's University
Kitauoyanishimachi, Nara 630-8506, Japan

[d] K. Ohkubo
Organization for Carbon Neutrality Collaboration (OCNC)
The University of Osaka
1–6 Yamada-oka, Suita, Osaka 565–0871, Japan

Supporting Information for this article is provided via a link at the end of the document.

Abstract: A versatile synthetic strategy for 3-azafluorenone derivatives was developed. The strategy enabled efficient access to previously inaccessible structural analogs. Crucially, *tert*-butyl protection of ketocarboxylic acid intermediates significantly improved isolated yields and enabled the incorporation of electron-donating, electron-withdrawing, and *π*-extended substituents. The photophysical properties of the compounds were characterized by UV–vis absorption and fluorescence spectroscopic measurements, and the electrochemical behavior was monitored using cyclic voltammetry. The electron-donating and *π*-extended substituents induced pronounced bathochromic shifts in absorption and emission, consistent with the narrowing of the HOMO–LUMO gap, whereas strong electron-withdrawing groups or 6-methoxy substitution caused a slight hypsochromic shift. Nitrogen incorporation and electron-withdrawing substituents stabilized the LUMO, affording more positive ground- and excited-state reduction potentials. Most derivatives exhibited higher excited-state reduction potentials than fluorenone, with the majority exceeding +1.6 V vs. SCE. Further, TD-DFT calculations reproduced the observed spectral trends and oscillator strengths, confirming the *π*–*π** nature of the lowest-energy transitions. All derivatives exhibited intense, red-shifted visible light absorption, and most showed high excited-state reduction potentials, demonstrating their potential for photoredox applications. These results establish detailed structure–property relationships for 3-azafluorenones, providing design principles for the rational tuning of optical and redox properties.

Introduction

Fluorenone is an aromatic ketone having a rigid *π*-conjugated scaffold and high structural stability, and has been widely applied in fluorescent dyes and electronic materials.[1–3] Owing to its absorption in the visible region and relatively long excited-state lifetime, fluorenone has also been employed as a visible-light-responsive photoredox catalyst.[4–11] Azafluorenones, which are structural analogs of fluorenones in which a part of the phenyl ring is replaced with a nitrogen atom, are expected to show distinct photophysical and electrochemical properties as a result of changess to the electronic structure after the introduction of a heteroatom.[12–16] In addition, the basicity and nucleophilicity of the ring nitrogen can be exploited to modulate their photophysical characteristics, offering

further potential for functional applications. To date, azafluorenone derivatives have been explored for use in amino acid-sensing probes,[17] organic light-emitting diodes (OLEDs),[18] and water-soluble imaging agents.[19,20] These studies underscore their potential as functional photoactive molecules, suggesting their broad utility in photoactive materials and molecular probe design.[21–23] Moreover, their demonstrated photoactivity suggests that azafluorenones could be promising scaffolds for light-driven catalytic transformations, such as photoredox catalysis.

In photoredox catalysis, the excited-state reduction potential critically depends on the electronic structure of the molecule. In azafluorenones, nitrogen incorporation is expected to stabilize the LUMO energy, thereby shifting the reduction potential positively.[15,16] This electronic modulation suggests that azafluorenones should exhibit catalytic activity comparable to or greater than that of fluorenones. In our previous study, we demonstrated that a 2-azafluorenone derivative could function as a photoredox catalyst.[24] However, its activation required short-wavelength irradiation, below 400 nm, raising concerns about side reactions and over-reduction. In general, photocatalysts capable of utilizing long-wavelength visible light are more advantageous in terms of reaction selectivity and substrate scope.[25] Therefore, to develop azafluorenone derivatives as practical photoredox catalysts, it is essential to develop new analogs that efficiently absorb long-wavelength light. Furthermore, to establish a rational design strategy, systematic investigations into how substituents and structural variations influence the photophysical and redox properties are necessary, along with the development of versatile synthetic methods for modular scaffold construction.

The classical synthetic method for azafluorenones involves Friedel–Crafts acylation; however, this approach requires cyclization from the pyridine ring side. Owing to the limited accessibility of pyridine carboxylic acid precursors, this strategy poses significant challenges for the synthesis of structurally diverse derivatives (Figure 1a).[26–29] To address this limitation, Laha et al. developed cyclization strategies from the phenyl ring (Figure 1b), [30–32] whereas Tu[33] and Scheerer[34] synthesized azafluorenones via the construction of a pyridine ring from 2,3-dihydro-1*H*-inden-1-one. These groups reported multiple synthetic routes that enabled the construction of various azafluorenone scaffolds. These advances have expanded the scope of accessible derivatives and provided a platform for investigating their functional properties. Nevertheless, although the photophysical properties of certain azafluorenone derivatives have been studied, systematic investigations of the effects of changes in the position of functional group substitutions on the molecular electronic structures and optical properties are still limited.[21,22,24,35,36]

In this study, we focused on 3-azafluorenone, among the four possible isomers with nitrogen atoms at the 1-, 2-, 3-, or 4-positions, considering its application as a photocatalyst. Further, 3-azafluorenone has been reported to absorb longer-wavelength visible light than that of other azafluorenones[21,22,24,35,36] and is predicted by density functional theory (DFT) calculations to absorb efficiently in the long-wavelength region of the visible spectrum (Figure 1c). Therefore, a new strategy for the synthesis of 3-azafluorenones with various substituent patterns was proposed, and three novel 3-azafluorenones were obtained in synthetically useful yields. The optical properties of the synthesized compounds were evaluated using UV–vis absorption, fluorescence, and phosphorescence measurements, and their electrochemical behavior was investigated using cyclic voltammetry (CV). Finally, the excited-state energy levels and reduction potentials of the derivatives were determined from these measurements.

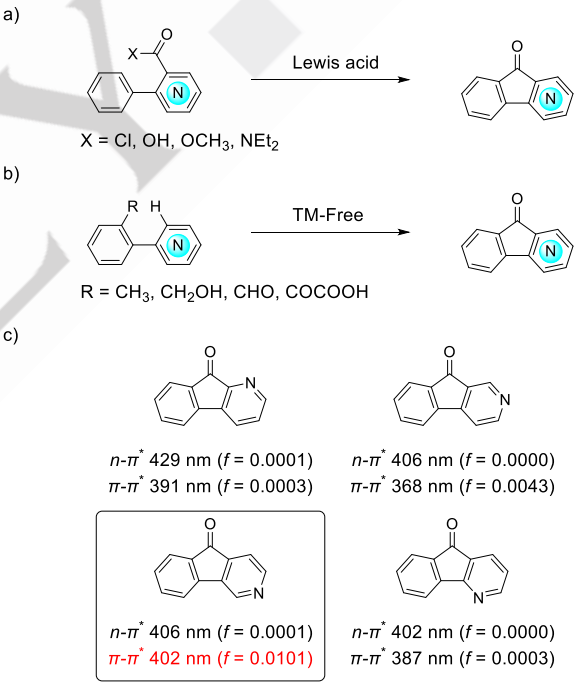


Figure 1. (a) Classical synthesis of azafluorenones. (b) Laha's synthesis of azafluorenones. (c) Calculated absorption wavelengths of azafluorenones. TM = transition metal.

Results and Discussion

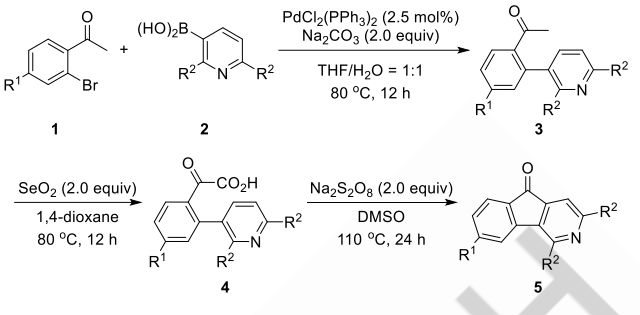
Synthesis

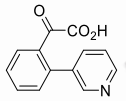
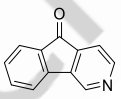
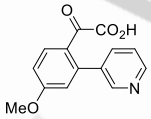
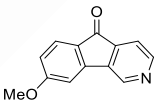
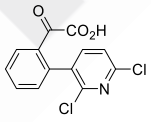
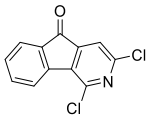
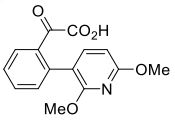
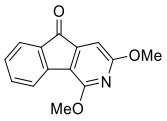
3-Azafluorenone (**5aa**) was synthesized according to the method reported by Laha et al. (Table 1). A Suzuki–Miyaura cross-coupling reaction between 1-(2-bromophenyl)ethan-1-one (**1a**) and 3-pyridylboronic

acid (**2a**) was conducted using $PdCl_2(PPh_3)_2$ as a catalyst in a tetrahydrofuran (THF)/water mixture. Upon reaction completion, the desired biaryl intermediate **3aa** was obtained. The oxidation of **3aa** with SeO_2 afforded the corresponding ketocarboxylic acid (**4aa**), which underwent a Minisci-type intramolecular cyclization to furnish the 3-azafluorenone core. The overall yield of **5aa** over three steps was 18%. To explore a "push−pull" structure containing a methoxy group as an electron-donating substituent at the 6-position and the pyridine nitrogen as an electron-withdrawing site at the 3-position, the synthesis of compound **5ba** was attempted. "Push–pull" aryl ketones have been reported to be effective photoinduced hydrogen atom transfer (HAT) catalysts.[37–39] Starting with 1-(2-bromo-4-methoxyphenyl)ethan-1-one (**1b**), Suzuki–Miyaura coupling, oxidation, and cyclization afforded **5ba** in an overall yield of 2.3%. The relatively low yield of **5ba** compared to **5aa** can be attributed to the low efficiency of the oxidation reaction with SeO_2. Pyridine rings tend to undergo radical addition at the C2, C4, and C6 positions, particularly upon the formation of pyridinium salts.[40–42] Introducing substituents at these positions may suppress undesired radical reactions and prevent structural degradation. Subsequently, we attempted to synthesize 3-azafluorenone derivatives **5ab** and **5ac** bearing chloro and methoxy groups at the 2- and 4-positions, respectively. We conducted the same three-step procedure using 2,4-dichloro- (**2b**) and 2,4-dimethoxypyridine boronic acids (**2c**) as starting materials; **5ab** was obtained in 1.9% overall yield, but **5ac** was not obtained. Some aromatic substrates bearing methoxy groups are known to undergo side reactions under SeO_2 oxidation conditions, often resulting in complex product mixtures and significantly reduced yields, accounting for the failure to obtain **5ac** in the present study. [43,44]

As an alternative route, the synthetic sequence was reconsidered with the hypothesis that ketocarboxylic acids could be synthesized by first performing the SeO_2 oxidation of **1a**, followed by a Suzuki–Miyaura coupling (Scheme S1). However, the coupling reaction did not proceed smoothly under these conditions, presumably because of the decarboxylation of the carboxyl group in the presence of a palladium catalyst.[45,46] To address this issue, a protective strategy using *tert*-butyl 2-(2-bromophenyl)-2-oxoacetate (**6a**) as the starting material was examined (Table 2). The Suzuki–Miyaura coupling of **6a** with various substituted pyridine boronic acids (**2ab**–**2af**) afforded the corresponding biaryl intermediates. Subsequent acid treatment removed the *tert*-butyl protecting group, and ketocarboxylic acids (**4ab**–**4af**) were obtained by adjusting the aqueous layer to pH 4–5 using a Na_2CO_3 solution.[47] Subsequent cyclization of the resulting acids yielded **5ab** (6.0%) and **5ac** (43%), resulting in significant improvements in yield.

Table 1. Synthesis of 3-azafluorenones via a reported synthetic route.



Compound	**4** (two-step yield)	**5** (three-step yield)
R^1 = H, R^2 = H	 **4aa** (72%)	 **5aa** (18%)
R^1 = OMe, R^2 = H	 **4ba** (20%)	 **5ba** (2.3%)
R^1 = H, R^2 = Cl	 **4ab** (7.6%)	 **5ab** (1.9%)
R^1 = H, R^2 = OMe	 **4ac** (not isolated)	 **5ac** (not isolated)

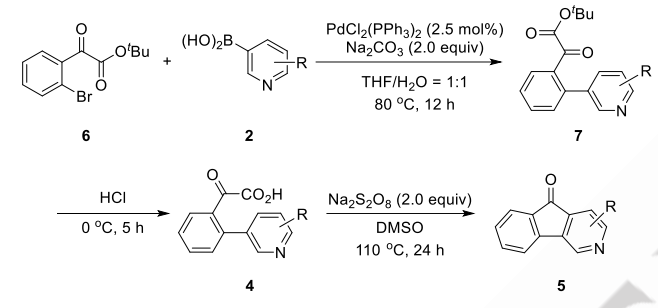
Isolated yields shown. Yield given as total yield.

The relatively low yield of **5ab** was attributed to the low efficiency of the Suzuki-Miyaura coupling in the first step. This improved strategy enabled the synthesis of other 3-azafluorenone derivatives. Compound **5ad**, bearing a quinoline ring, was obtained in 16% yield; **5ae**, bearing a propynyl group at the 1-position, was obtained in 17% yield; and **5af**, bearing a trifluoromethyl group at the 2-position, was obtained in 35% yield. Notably, **4af** was obtained in nearly quantitative yield, suggesting that this synthetic route is a useful new approach.

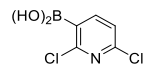
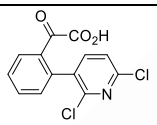
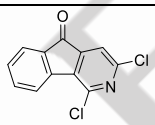
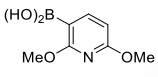
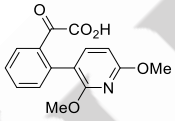
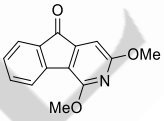
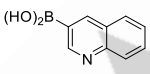
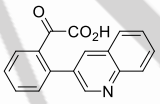
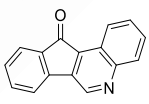
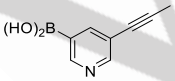
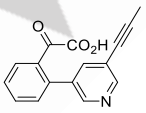
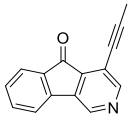
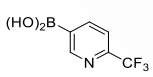
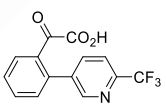
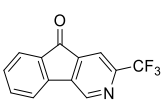
The structures of compounds **5aa**, **5ab,** and **5ac** were confirmed by X-ray diffractometry (XRD) analysis (Figure 2). According to single-crystal XRD analyses, the 3-azafluorenone scaffold remained planar in all derivatives. In addition, **5aa** has a C=O bond length of 1.218 Å, and the C–N bonds measure 1.340 Å and 1.346 Å, shorter than the other C–C bonds (≈ 1.377–1.414 Å). In contrast, **5ab** contains a distorted pyridine

ring because of the influence of the chloro substituents, with the bond angles ranging from 114.70° to 125.47°, deviating from the ideal 120°. In **5ac**, the methoxy groups are effectively conjugated with the *π*-system, as indicated by the aryl–O bond length (1.358 Å), which is comparable to that typically observed in conjugated methoxy-substituted pyridines,[48] and by the nearly coplanar orientation of the methoxy substituents. Consistently, DFT calculations reproduced these structural features, giving C=O bond lengths of 1.21 Å for all derivatives, C–N bond lengths of 1.34 and 1.33 Å for **5aa**, and an aryl–O bond length of 1.35 Å for the methoxy group, in close agreement with the experimental values.

Table 2. Synthesis of 3-azafluorenones via the *tert*-butyl protection strategy.



6 2 7 4 5

2	4 (two-step yield)	5 (three-step yield)
	 **4ab** (24%)	 **5ab** (6.0%)
	 **4ac** (84%)	 **5ac** (43%)
	 **4ad** (27%)	 **5ad** (16%)
	 **4ae** (72%)	 **5ae** (17%)
	 **4af** (>99%)	 **5af** (35%)

Isolated yields shown. Yield given as total yield.

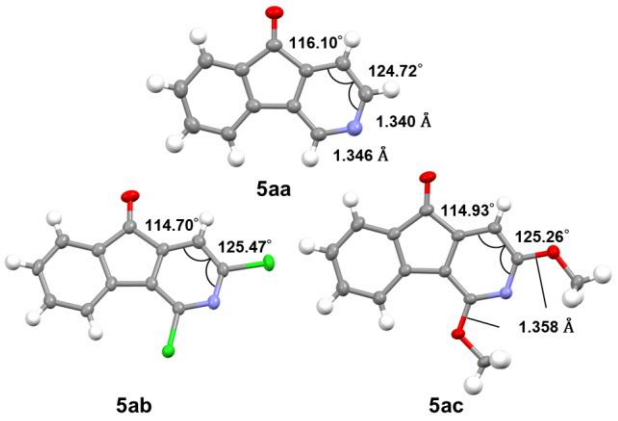


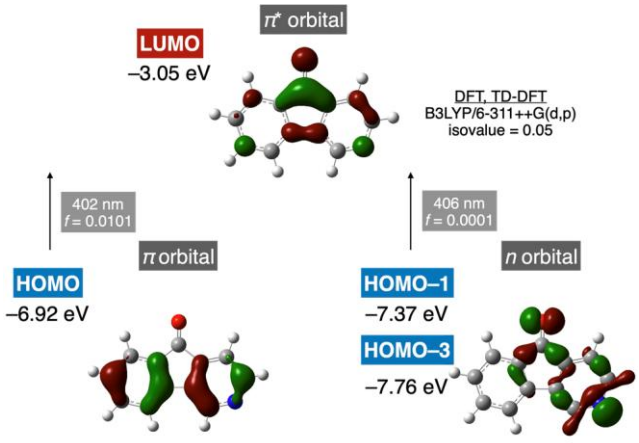
Figure 2. X-ray crystal structures of **5aa**, **5ab,** and **5ac**.

DFT calculations

Geometry optimization was performed using DFT at the B3LYP/6-311++G(d,p) level of theory. Time-dependent DFT (TD-DFT) calculations were subsequently performed on the optimized structures to determine their electronic absorption wavelengths and oscillator strengths (*f*) (Table 3). The overall electronic structure of **5aa** was found to be similar to that of fluorenone. The visible absorption band of **5aa** was primarily attributed to a *π*–*π** transition. The LUMO was mainly localized on the carbonyl group, whereas the HOMO was delocalized over the aromatic ring. The limited spatial overlap between these orbitals results in a small oscillator strength, which accounts for weak absorption. A weak *n*–*π** transition was also identified, originating from mixed excitations involving the HOMO–1 and HOMO–3 orbitals through configuration interaction. As a result of this mixing, the *n*–*π** transition appears at a longer wavelength than the *π*–*π** transition. However, the limited orbital overlap between the nonbonding and *π** orbitals leads to a very small oscillator strength (*f* = 0.0001), indicating only a minor contribution to absorption. For **5ab**, the introduction of the electron-withdrawing chloro groups lowered both the HOMO and LUMO energies. Specifically, the *π*–*π** transition was red-shifted to 422 nm (*f* = 0.0256). For **5ac**, the electron-donating methoxy groups increased the HOMO energy, further narrowing the HOMO–LUMO gap and resulting in a *π*–*π** transition at 475 nm (*f* = 0.0348). For **5ad**, extended *π*-conjugation stabilized the LUMO relative to the HOMO, leading to a red-shifted *π*–*π** transition at 471 nm (*f* = 0.0057). Further, **5ae** showed a *π*–*π** transition at 404 nm (*f* = 0.0372), whereas **5af** showed a *π*–*π** transition at 398 nm (*f* = 0.0152) because of the strong electron-withdrawing trifluoromethyl group, thus lowering the HOMO energy. For **5ba**, the 6-methoxy substituent slightly increased the HOMO energy, resulting in a *π*–*π** transition at 409 nm (*f* = 0.0135), indicating a minor effect on absorption. Overall, these results indicate that the visible absorption of these 3-azafluorenone derivatives originates predominantly

from π–π^* transitions, with substituents modulating the HOMO and LUMO energies and thus the transition energies (Table 3).

Table 3. DFT-calculated frontier orbitals and low-energy electronic transitions of 3-azafluorenones.



Compound	HOMO-1 /eV (*n* orbital)	HOMO/eV (π orbital)	LUMO/eV (π^* orbital)	$\lambda_{abs,max}$/nm (*f*)
Fluorenone	−7.21	−6.59	−2.66	*n*-π^* 392 (0.0000) π-π^* 396 (0.0035)
5aa	−7.37	−6.92	−3.05	*n*-π^* 406 (0.0001) π-π^* 402 (0.0101)
5ab	−7.86	−7.06	−3.41	*n*-π^* 394 (0.0000) π-π^* 422 (0.0256)
5ac	−7.28	−6.02	−2.73	*n*-π^* 402 (0.0000) π-π^* 475 (0.0348)
5ad	−7.25 (HOMO-2)	−6.50	−3.18	*n*-π^* 431 (0.0000) π-π^* 471 (0.0057)
5ae	−7.04	−6.70	−2.97	*n*-π^* 427 (0.0000) π-π^* 404 (0.0372)
5af	−7.80	−7.32	−3.43	*n*-π^* 409 (0.0000) π-π^* 398 (0.0152)
5ba	−7.26	−6.60	−2.86	*n*-π^* 399 (0.0001) π-π^* 409 (0.0135)

Photophysical and electrochemical properties

Next, the UV–vis absorption spectra of **5aa**–**5af**, **5ba**, and fluorenone were recorded to evaluate the optical properties of the 3-azafluorenone derivatives (Figure 3). Compound **5aa** showed the maximum absorption of the derivatives at 400 nm, corresponding to a red shift relative to fluorenone. The experimentally observed absorption wavelength of **5aa** was consistent with the DFT-calculated values and reported data.[35,36] Experimentally, **5ab** and **5ac** showed further red-shifted absorption (410 and 466 nm, respectively) compared to **5aa**, consistent with the calculated values (422 and 475 nm). The experimental oscillator strengths were approximately two and three times those of **5aa**, consistent with the trends predicted by theory. Compared to that of **5aa**, the absorption of **5ad** was red-shifted to 423 nm, although the extent of this shift was smaller than the calculated value (471 nm). This discrepancy may arise from deviations from planarity or solvation effects, which reduce effective conjugation in solution. In contrast, the maximum absorption of **5ae** (407 nm vs. calc. 404 nm) and **5af** (387 nm vs. calc. 398 nm) agree with the calculated values. The experimental absorption of **5ba** occurred at 390 nm, a slight blue shift relative to that of **5aa**. The calculated absorption wavelength was slightly red-shifted to 409 nm. This discrepancy is likely due to structural constraints: the 6-methoxy group is positioned such that its lone pair does not effectively conjugate with the π-system, limiting delocalization. Such positional effects of electron-donating substituents on conjugation have been reported for fluorenone derivatives,[49] indicating that the extent of the red-shift can be modulated by substituent placement.

Next, the fluorescence spectra of **5aa**–**5af**, **5ba**, and fluorenone were recorded using their respective absorption maxima as excitation wavelengths to evaluate the fluorescence properties of the 3-azafluorenone derivatives (Figure 4). Compound **5aa** produced an emission maximum at 505 nm, comparable to that of fluorenone. In contrast, **5ab**, **5ac** and **5ad** showed further red-shifted emissions compared to those of **5aa**, consistent with the red-shifts observed in their absorption spectra and attributable to the stabilization of the excited state resulting from a narrower HOMO–LUMO gap. **5af** exhibited slightly blue-shifted emissions relative to **5aa**, consistent with the blue shifts observed in their UV–vis absorption spectra. In contrast, compound **5ba** showed a minor red shift compared to **5aa**; however, the magnitude of this shift was significantly smaller than that of **5ac**, which bears methoxy substituents at the 2- and 4-positions. As discussed above, this behavior can be attributed to the methoxy group at the 6-position, whose lone pair

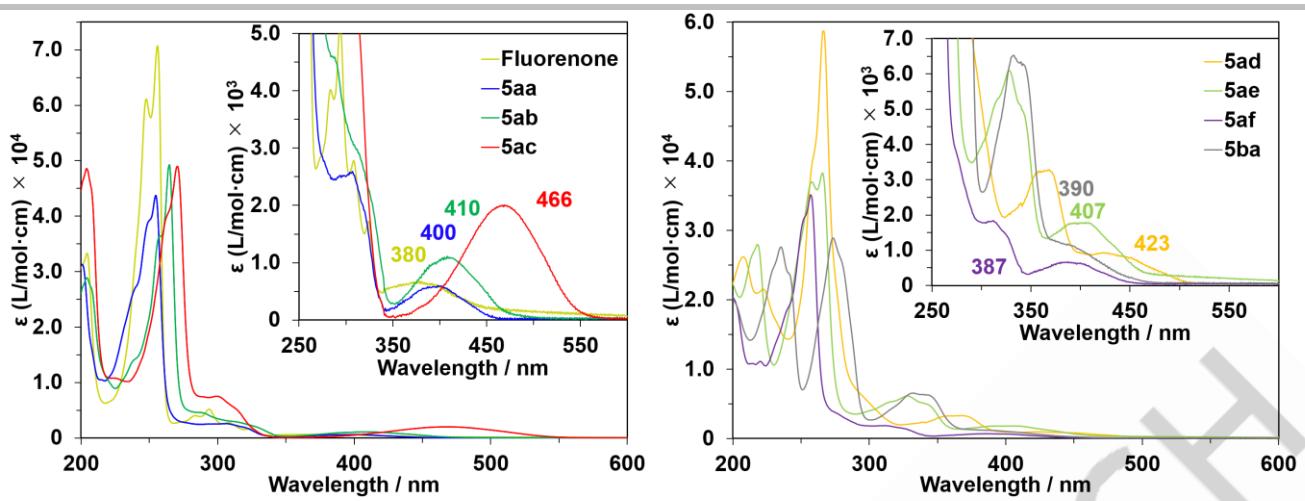


Figure 3. Absorption spectra of fluorenone, **5aa**-**5ac** (left) and **5ad**-**5af**, **5ba** (right) in MeCN (0.02 mM).

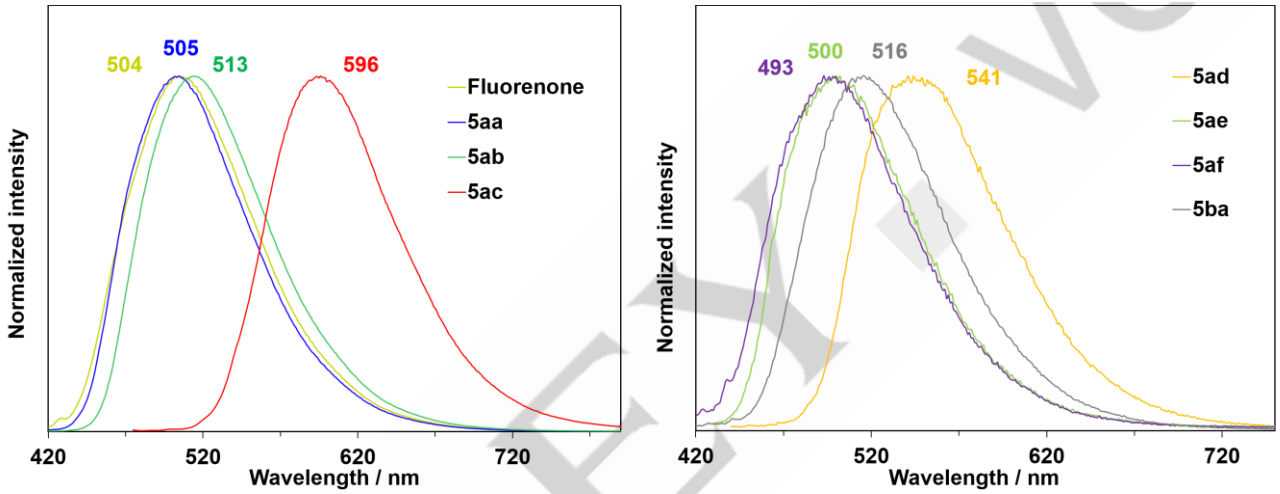


Figure 4. Fluorescence spectra of fluorenone, **5aa**-**5ac** (left) and **5ad**-**5af**, **5ba** (right) in MeCN (0.5 mM).

cannot effectively conjugate with the *π*-system, resulting in restricted electronic delocalization.

CV measurements were performed to evaluate the ground-state reduction potentials of **5aa**–**5af**, **5ba**, and fluorenone (Figure 5). All 3-azafluorenone derivatives exhibited reversible redox waves. Compared to fluorenone, the incorporation of a nitrogen atom resulted in a pronounced positive shift in the reduction potential, indicating enhanced electron-accepting ability. Compound **5aa** displayed a reduction potential of −1.06 V vs. the saturated calomel electrode (SCE), whereas **5ab** showed a slight positive shift (−1.04 V vs. SCE), consistent with LUMO stabilization by the electron-withdrawing chloro substituent. In contrast, **5ac** showed a marked negative shift (−1.15 V vs. SCE), suggesting LUMO destabilization induced by the electron-donating methoxy group, making reduction more difficult. In contrast, **5ad** exhibited a significantly more positive potential (−0.94 V vs. SCE), reflecting strong electron-accepting character, likely arising from the extended *π*-conjugation. Although the calculated LUMO energy of **5ad** (−3.18 eV) is slightly higher than that of **5ab** (−3.41 eV), the more positive reduction potential observed for **5ad** suggests that stabilization of the radical anion through delocalization following one-electron reduction also plays a significant role in determining the redox behavior. The potential of **5ae** was comparable to that of **5aa** (−1.05 V vs. SCE), indicating that the conjugative effect of the alkynyl group is counterbalanced by the electronegativity and weak electron-donating nature of the sp-hybridized carbon. The most positive shift was observed for **5af** (−0.92 V vs. SCE), consistent with strong LUMO stabilization by the electron-withdrawing trifluoromethyl group through inductive effects. In contrast, **5ba** exhibited the most negative reduction potential (−1.19 V vs. SCE), indicating reduced electron affinity, likely because of the limited conjugative overlap between the methoxy group at the 6-position and the *π*-system, which instead increases local electron density and destabilizes the LUMO.

The photophysical properties of **5aa**–**5af**, **5ba**, and fluorenone are summarized in Table 4. Among these, fluorenone exhibited the longest fluorescence lifetime (τ = 16.2 ns) in the singlet excited state. All 3-

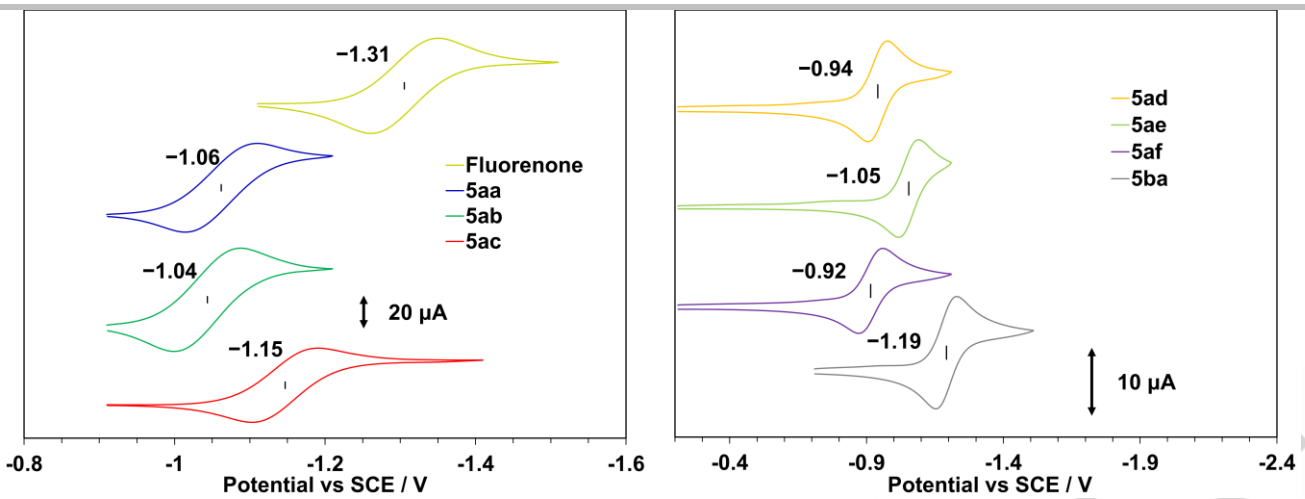


Figure 5. Cyclic voltammograms of fluorenone, **5aa-5ac** (left), **5ad-5af**, and **5ba** (right) in MeCN (1.0 mM). Vertical lines denote half-wave potential.

azafluorenone derivatives showed shorter lifetimes compared to fluorenone. Among them, **5aa** displayed the longest lifetime (τ = 6.56 ns) with a relatively high quantum yield (Φ_f = 0.30), followed by **5ab** (τ = 4.57 ns, Φ_f = 0.29). Moderate lifetimes and lower emission efficiencies were observed for **5ad** (τ = 3.49 ns, Φ_f = 0.10), **5af** (τ = 2.14 ns, Φ_f = 0.11), and **5ba** (τ = 3.31 ns, Φ_f = 0.15). In contrast, **5ac** (τ = 0.27 ns, Φ_f = 0.01) and **5ae** (τ = 0.86 ns, Φ_f = 0.05) exhibited very short lifetimes and drastically suppressed fluorescence.

The ground- and singlet-excited-state reduction potentials, together with the experimental singlet excitation energies, are listed in Table 5. The calculated singlet and triplet excitation energies are also included in the same table. The excited-state reduction potential is a key parameter for assessing the photochemical driving force and the feasibility of photoinduced electron transfer, thereby serving as a crucial design guideline for photocatalysts and other functional materials. Compound **5aa** yielded a singlet excited-state reduction potential of +1.72 V vs. SCE, significantly higher than that of fluorenone (+1.56 V vs. SCE), indicating markedly enhanced reducing power and strong potential for photoredox applications. The calculated singlet and triplet excitation energies for **5aa** were 2.64 and 1.54 eV, respectively, compared to 2.67 and 1.59 eV for fluorenone. **5ab** showed a slightly lower value (+1.68 V vs. SCE) but maintained sufficient reducing ability, with calculated singlet and triplet energies of 2.51 and 1.47 eV, respectively. In contrast, **5ac** showed a substantial decrease to +1.23 V vs. SCE in the singlet state, accompanied by lower calculated singlet and triplet energies (2.25 and 1.33 eV, respectively), suggesting significantly decreased electron-accepting capacity. These results suggest that the introduction of electron-donating groups destabilized the LUMO, reducing the excited-state reduction potential. Compound **5ad** (+1.67 V vs. SCE) showed a slightly lower value compared to **5aa**, with calculated singlet and triplet excitation energies of 2.23 and 1.18 eV, respectively. The alkynyl-substituted compound **5ae** (+1.71 V vs. SCE) displayed an almost identical

Table 4. Photophysical properties of 3-azafluorenones.

Compound	$\lambda_{abs,max}$/nm	$\lambda_{flu,max}$/nm	Φ_f	τ/ns
Fluorenone	380	504	0.32	16.2
5aa	400	505	0.30	6.56
5ab	410	513	0.29	4.57
5ac	466	596	0.01	0.27
5ad	423	541	0.10	3.49
5ae	407	500	0.05	0.86
5af	387	493	0.11	2.14
5ba	390	516	0.15	3.31

Table 5. Reduction potentials of 3-azafluorenones.

Compound	Reduction potential vs. SCE /V		$^1E^*$[c] /eV	$^1E^*$(calc)[d] /eV	$^3E^*$(calc)[e,f] /eV
	E_{red}[a]	$^1E_{red}^*$[b]			
Fluorenone	−1.31	+1.56	2.86	2.67	1.59
5aa	−1.06	+1.72	2.78	2.64	1.54
5ab	−1.04	+1.68	2.72	2.51	1.47
5ac	−1.15	+1.23	2.37	2.25	1.33
5ad	−0.94	+1.67	2.61	2.23	1.18
5ae	−1.05	+1.71	2.77	2.68	1.96
5af	−0.92	+1.95	2.86	2.84	1.55
5ba	−1.19	+1.60	2.79	2.64	1.67

[a] Ground state reduction potential. [b] Reduction potential of the singlet excited state. [c] Singlet excited energy determined from the Frank–Condon principle to be $^1E^* = (h\nu + h\nu')/2$, where $h\nu$ and $h\nu'$ are energies of absorption and fluorescence maxima. [d] Singlet excited energy determined by TD-DFT calculations. [e] Triplet-excited energy determined by TD-DFT calculations. [f] No phosphorescence was experimentally observed at 77 K due to strong delay fluorescence (Figures S2 and S3).[50-52]

potential to **5aa**, highlighting that the *π*-conjugation effect of the alkyne group is offset by its weak electron-withdrawing character. The calculated singlet and triplet excitation energies were 2.68 and 1.96 eV, respectively. The highest potential was observed for **5af** (+1.95 V vs. SCE), attributable to the strong electron-withdrawing effect of the trifluoromethyl group and the consequent LUMO stabilization; its calculated singlet and triplet excitation energies were 2.84 and 1.55 eV, respectively. The methoxy-substituted compound **5ba** (+1.60 V vs. SCE) exhibited a lower potential than **5aa**, consistent with LUMO destabilization induced by the electron-donating nature of the methoxy group, which decreases the oxidizing power of the excited state. The calculated singlet and triplet excitation energies were 2.64 and 1.67 eV, respectively. Collectively, these findings demonstrate that both the extent of *π*-conjugation and the electronic characteristics of substituents play decisive roles in tuning the excited-state redox properties of the azafluorenone scaffold.

Conclusion

A novel synthetic strategy for 3-azafluorenone derivatives was developed, enabling the efficient preparation of structurally diverse compounds that were previously difficult to access. Optimization of the reaction sequence, particularly through *tert*-butyl protection of the ketocarboxylic acid intermediates, significantly improved the overall yield and substrate scope. Systematic investigations of the effects of the substituent position and electronic properties on the photophysical and electrochemical behavior of the derivatives were conducted. Photophysical analyses revealed that electron-donating and-*π*-conjugated substituents led to absorption and fluorescence at longer wavelengths compared to parent fluorenones, consistent with the narrowing of the HOMO–LUMO gap. In contrast, the introduction of a methoxy group at the 6-position or a strongly electron-withdrawing substituent such as a trifluoromethyl group at the 2-position caused a shift toward shorter wavelengths, indicating that both the electronic characteristics and substitution pattern affect the optical properties significantly. CV measurements revealed that LUMO stabilization was achieved through *π*-conjugation extension and the incorporation of electron-withdrawing groups, leading to more positive ground-state reduction potentials. Similar trends were observed for the excited-state reduction potentials, highlighting the high electron-accepting ability of the 3-azafluorenone derivatives and their potential applicability in photoredox catalysis. Importantly, the newly synthesized 3-azafluorenone derivatives absorbed visible light, further broadening their applicability and opening opportunities for use in visible-light-driven photocatalysis and related optoelectronic applications. Overall, these findings demonstrated that 3-azafluorenone derivatives are a versatile basis for preparing tunable photoactive molecules. Crucially, their optical and redox properties can be finely tuned via rational molecular design, underscoring their potential for photocatalysis and related applications.

Supporting Information

The authors have cited additional references in the Supporting Information.[32, 53, 54] Supporting Information contains all relevant synthetic procedures and corresponding NMR spectra. crystallographic details are provided in the Supporting Information, and the CCDC numbers are listed in Table S1.[55]

Acknowledgements

This study was supported by Japan Science and Technology Agency (JST) SPRING (grant number JPMJSP2138 to T.K.) and JSPS KAKENHI Grants (JP23K13709 to Y.I. , JP24K21770 to K.O.). We thank Dr. Takanori Nakane and Prof. Genji Kurisu for supporting X-ray crystallographic analyses at the Institute of Protein Research, The University of Osaka.

Conflict of Interest

The authors declare no conflict of interest.

Data Availability Statement

The data supporting the findings of this study are available from the corresponding author upon reasonable request**.** The raw diffraction images of compound **5ab** were deposited using XRDa (accession code XRD-00421).

Keywords: 3-Azafluorenone • Emission properties • Redox potential • Excited state properties

[1] S. Semin, X. Li, Y. Duan, T. Rasing, “Nonlinear Optical Properties and Applications of Fluorenone Molecular Materials” *Adv. Opt. Mater.* **2021***, 9,* 2100327.

[2] A. L. Capodilupo, V. Vergaro, E. Fabiano, M. D. Giorgo, F.Baldassarre, A. Cardone, A. Maggiore, V. Maiorano, D. Sanvitto, G. Gigli, G. Ciccarella, “Design and synthesis of fluorenone-based dyes: two-photon excited fluorescent probes for imaging of lysosomes and mitochondria in living cells” *J. Mater. Chem. B* **2015**, *3*, 3315.

[3] J. Lee, T. Sakaguchi, G. Kwak, “Thermodynamic Fluorescence Behavior of a Fluorenone Derivative through Solvent- and Temperature-Controlled Hydrogen Bonding” *ChemPhotoChem* **2025**, *9*, e202400314.

[4] J. Kollmann, Y. Zhang, W. Schilling, T. Zhang, D. Riemer, S. Das, “A simple ketone as an efficient metal-free catalyst for

visible-light-mediated Diels–Alder and aza-Diels–Alder reactions" *Green Chem*. **2019**, *21*, 1916.

[5] W. Schilling, D. Riemer, Y. Zhang, N. Hatami, S. Das, "Metal-Free Catalyst for Visible-Light-Induced Oxidation of Unactivated Alcohols Using Air/Oxygen as an Oxidant" *ACS Catal*. **2018**, *8*, 5425.

[6] P. P. Khobrekar, V. R. Chari, S. T. Bugde, "9-Fluorenone Catalyzed Visible Light Oxidation of Hydrazides: An Efficient Route for the Synthesis of *N*,*N*'-Diacylhydrazines Derivatives" *ChemistrySelect* **2024**, *9*, e202401316.

[7] J.-B. Xia, C. Zhu, C. Chen, "Visible Light-Promoted Metal-Free C−H Activation: Diarylketone Catalyzed Selective Benzylic Mono- and Difluorination" *J. Am. Chem. Soc*. **2013**, *135*, 17494.

[8] N. A. Romero, D. A. Nicewicz, "Organic Photoredox Catalysis" *Chem. Rev*. **2016**, *116*, 10075.

[9] K. Ohkubo, S. Matsumoto, H. Asahara, S. Fukuzumi, "9-(4-Halo-2,6-xylyl)-10-methylacridinium Ion as an Effective Photoredox Catalyst for Oxygenation and Trifluoromethylation of Toluene Derivatives" *ACS Catal.* **2024**, *14*, 2671.

[10] Y. Tajimi, Y. Nachi, R. Inada, R.Hashimoto, M. Yamawaki, K. Ohkubo, T. Morita, Y. Yoshimi, "9-Cyano-10-methoxycarbonylanthracene as a Visible Organic Photoredox Catalyst in the Two-Molecule Photoredox System" *J. Org. Chem*. **2022**, *87*, 7405.

[11] T. Kodama, M. Kubo, W. Shinji, K. Ohkubo, M. Tobisu, "Phenylene-bridged Bis(benzimidazolium) (BBIm2+): A Dicationic Organic Photoredox Catalyst" *Chem. Sci.* **2020**, *11*, 12109.

[12] K. Tokuo, H. Sakai, T. Sakanoue, T. Takenobu, Y. Araki, T. Wada, T. Hasobe, "Control of the electrochemical and photophysical properties of *N*-substituted benzo[*ghi*]perylene derivatives" *Mater. Chem. Front*. **2017**, *1*, 2299.

[13] J. M. Lim, S. Shim, H. T. Bui, J. Kim, H.-J. Kim, Y. Hwa, S. Cho, "Substitution Effect of a Single Nitrogen Atom on π-Electronic Systems of Linear Polycyclic Aromatic Hydrocarbons (PAHs): Theoretically Visualized Coexistence of Mono- and Polycyclic π-Electron Delocalization" *Molecules* **2024**, *29*, 784.

[14] S. Slimak, A. Lietard, K. D. Jordan, J. R. R. Verlet, "Effect of N Atom Substitution on Electronic Resonances: A 2D Photoelectron Spectroscopic and Computational Study of Anthracene, Acridine, and Phenazine Anions" *J. Phys. Chem. A* **2024**, *128*, 5321.

[15] E. R. Darzi, D. A. Stanfield, L. Mcdermott, A. V. Kelleghan, B. J. Schwartz, N. K. Garg, "Facile synthesis of 2-aza-9,10-diphenylanthracene and the effect of precise nitrogen atom incorporation on OLED emitters performance" *Mater. Adv*. **2023**, *4*, 3351.

[16] K. Górski, K. Noworyta, J. Mech-Piskorz, "Influence of the heteroatom introduction on the physicochemical properties of 5-heterotruxenes containing nitrogen, oxygen and sulfur atom" *RSC Adv*. **2020**, *10*, 42363.

[17] R. Grigg, T. Mongkolaussavaratana, C. A. Pounds, S. Sivagnanam, "1,8-Diazafluorenone and related-compounds-a new reagent for the detection of alpha-amino-acids and latent fingerprints" *Tetrahedron Lett.* **1990**, 31, 7215.

[18] X.-Y. Liu, Y.-J. Zhang, X. Fei, Q. Ran, M.-K. Fung, J. Fan, "Diazaspirocycles: novel platforms for efficient phosphorescent organic light-emitting diodes" *J. Mater. Chem. C* **2019**, *7*, 1370.

[19] M. Gao, H.F. Su, Y.H. Lin, X. Ling, S.W. Li, A.J. Qin, B.Z. Tang, "Photoactivatable aggregation-induced emission probes for lipid droplets-specific live cell imaging" *Chem. Sci.* **2017**, *8*, 1763.

[20] A. Sharma, S. Umar, P. Kar, K. Singh, M. Sachdev, A. Goel, "A new type of biocompatible fluorescent probe AFN for fixed and live cell imaging of intracellular lipid droplets" *Analyst* **2016**, *141*, 137.

[21] M. Cigáň, P. Danko, H. Brath, M. Čakurada, R. Fišera, J. Donovalová, J. Filo, M. Weis, J. Jakabovič, M. Novota, A. Gáplovský, "4-Azafluorenone and α-Carboline Fluorophores with Green and Violet/Blue Emission" *Molecules* **2019**, *24,* 2378.

[22] N. H. Angello, R. E. Wiley, C. J. Abelt, J. R. Scheere, "Synthesis and Spectrophotometric Analysis of 1-Azafluorenone Derivatives" *Molecules* **2020**, *25,* 3358.

[23] J. Orrego-Hernandez, C. Lizarazo, J. Cobo, J. Portilla, "Pyrazolo-fused 4-azafluorenones as key reagents for the synthesis of fluorescent dicyanovinylidenesubstituted derivatives" *RSC Adv*. **2019**, *9*, 27318.

[24] H. Asahara, Y. Horikawa, K. Iwai, N. Nishiwaki, K. Ohkubo, "2-Azafluorenone derivatives: Photocatalyst for oxygenation of toluene via electron transfer and hydrogen-atom transfer" *J. Photochem. Photobiol. A Chem.* **2023***, 15,* 100184.

[25] L. Marzo, S. K. Pagire, O. Reiser, B. König, "Visible-Light Photocatalysis: Does It Make a Difference in Organic Synthesis?" *Angew. Chem. Int. Ed*. **2018**, *57*, 10034.

[26] M. T. DuPriest, C. L. Schmidt, D. Kuzmich, S. B. Williams, "A Facile Synthesis of 7-Halo-5H-indeno[1,2-b]pyridines and -pyridin-5-ones" *J. Org. Chem*. **1986,** *51*, 2021.

[27] R. Sreekmar, P. Rugmini, R. Padmakumar, "Synthesis of Azafluorenones using Zeolites" *Synth. Commun*. **1998**, *28*, 2071.

[28] M. Alessi, A. L. Larkin, K. A. Ogilvie, L. A. Green, S. Lai, S. Lopez, V. Snieckus, "Directed ortho Metalation-Boronation and Suzuki-Miyaura Cross Coupling of Pyridine Derivatives: A One-Pot Protocol to Substituted Azabiaryls" *J. Org. Chem*. **2007**, *72*, 1588.

[29] S. Zhang, L.-Y. Liao, F. Zhang, X.-F. Duan, "Arylation, Alkenylation, and Alkylation of 2-Halopyridine N-Oxides with Grignard Reagents: A Solution to the Problem of C2/C6 Regioselective Functionalization of Pyridine Derivatives" *J. Org. Chem*. **2013**, *78*, 2720.

[30] J. K. Laha, K. P. Jethava, S. Patel, "Scope of Successive C−H Functionalizations of the Methyl Group in 3-Picolines: Intramolecular Carbonylation of Arenes to the MetalFree Synthesis of 4-Azafluorenones" *Org. Lett*. **2015**, *17*, 5890.

[31] J. K. Laha, K. P. Jethava, S. Patel, K. V. Patel, "Intramolecular Acylation of Unactivated Pyridines or Arenes via Multiple C−H Functionalizations: Synthesis of All Four Azafluorenones and Fluorenones" *J. Org. Chem*. **2017**, *82*, 76.

[32] J. K. Laha, K. V. Patel, G. Dubey, K. P. Jethava, "Intramolecular Minisci acylation under silver-free neutral conditions for the synthesis of azafluorenones and fluorenones" *Org. Biomol. Chem*. **2017***, 15,* 2199.

[33] Y. Li, W. Fan, H.-W. Xu, B. Jiang, S.-L. Wang, S.-J. Tu, "A novel three-component [5 + 1] heterocyclization leading to 2-azafluorenone synthesis and its polyfunctionalizations" *Org. Biomol. Chem*. **2013**, *11*, 2417.

[34] V. A. Lehman, Y. Ma, J. R. Scheerer, "Construction of the 4-Azafluorenone Core in a Single Operation and Synthesis of Onychine" *J. Org. Chem*. **2024**, *89*, 11078.

[35] L. Biozók, "Photophysical properties of 3-azafluorenone" *Reac. Kinet. Mech. Catal.* **1997**, *61*, 57.

[36] L. Biozók, A. Cser, K. Nagy, "Substituent and solvent effects on the photophysical properties of 3-azafluorenone derivatives" *J. Photochem. Photobiol. A Chem.* **2001***, 146,* 59.

[37] Y. Shen, Y. Gu, R. Martin, "*sp*^{3} C−H Arylation and Alkylation Enabled by the Synergy of Triplet Excited Ketones and Nickel Catalysts" *J. Am. Chem. Soc.* **2018**, *140*, 12200.

[38] S. Xu, Y. Ping, W. Li, H. Guo, Y. Su, Z. Li, M. Wang, W. Kong, "Enantioselective C(sp^3)−H Functionalization of Oxacycles via Photo-HAT/Nickel Dual Catalysis" *J. Am. Chem. Soc*. **2023,** *145*, 5231.

[39] A. Luridiana, D. Mazzarella, L. Capaldo, J. A. Rincón, P. García-Losada, C. Mateos, M. O. Frederick, M. Nuño, W. J. Buma, T. Noël, "The Merger of Benzophenone HAT Photocatalysis and Silyl RadicalInduced XAT Enables Both Nickel-Catalyzed Cross-Electrophile Coupling and 1,2-Dicarbofunctionalization of Olefins" *ACS Catal.* **2022**, *12*, 11216.

[40] E. L. Saux, E. Georgiou, I. A. Dmitriev, W. C. Hartley, P. Melchiorre, "Photochemical Organocatalytic Functionalization of Pyridines via Pyridinyl Radicals" *J. Am. Chem. Soc.* **2023**, *145*, 47.

[41] Q. Shi, X. Huang, R. Yang, W. H. Liu, "Unified ionic and radical C-4 alkylation and arylation of pyridines" *Chem. Sci*. **2024**, *15*, 12442.

[42] M. Kim, Y. Koo, S. Hong, "*N*-Functionalized Pyridinium Salts: A New Chapter for Site-Selective Pyridine C−H Functionalization via Radical-Based Processes under Visible Light Irradiation" *Acc. Chem. Res*. **2022**, *55*, 3043.

[43] S. Morita, T. Yoshimura, J. Matsuo, "Intramolecular Büchner Reaction and Oxidative Aromatization with SeO_2 or O_2" *Chem. Pharm. Bull.* **2019**, *67*, 729.

[44] P. S. Hellwig, T. J. Peglow, F. Penteado, L. Bagnoli, G. Perin, E. Lenardão, "Recent Advances in the Synthesis of Selenophenes and Their Derivatives" *Molecules* **2020**, *25,* 5907.

[45] F. Bilodeau, M.-C. Brochu, N. Guimond, K. H. Thesen, P. Forgione, "Palladium-Catalyzed Decarboxylative Cross-Coupling ReactionBetween Heteroaromatic Carboxylic Acids and Aryl Halides" *J. Org. Chem.* **2010**, *75*, 1550.

[46] C. Peschko, C. Winklhofer, W. Steglich, "Biomimetic Total Synthesis of Lamellarin L by Coupling of Two Different Arylpyruvic Acid Units" *Chem. Eur. J.* **2000**, *6*, 1147.

[47] R. Gallagher, T. Qudah, T. Balle, M. Chebib, M. D. Mcleod, "Novel methyllycaconitine analogues selective for the α4β2 over α7 nicotinic acetylcholine receptors" *Bioorg. Med. Chem.* **2021**, *51*, 116516.

[48] M. Al-Refai, M. M. Ibrahim, A. Geyer, M. Marsch, B. F. Ali, "Synthesis, Spectroscopic Characterization and X-ray Structure Analysis of 6-(2,5-Dichlorothiophen-3-yl)-2-methoxy-4-(4-methoxyphenyl)pyridine-3-carbonitrile" *J. Chem. Crystallogr.* **2016**, *46*, 331.

[49] I. Ghosh, A. Mukhopadhyay, A. L. Koner, S. Samanta, W. M. Nau, J. N. Moorthy, "Excited-state properties of fluorenones: influence of substituents, solvent and macrocyclic encapsulation" *Phys. Chem. Chem. Phys*. **2014**, *16*, 16436.

[50] R. Zwarich, "A Study of the Excited Electronic States of 9-Fluorenone" *J. Mol. Spectrosc.* **1974**, *52*, 329.

[51] J. Köhler, P. Hemberger, I. Fischer, G. Piani, L. Poisson, "Ultrafast Dynamics of Isolated Fluorenone" *J. Phys. Chem. A* **2011**, *115*, 14249.

[52] B. Soep, J. M. Mestdagh, M. Briant, M. A. Gaveau, L. Poisson, "Direct observation of slow intersystem crossing in an aromatic ketone, fluorenone" *Phys. Chem. Chem. Phys.* **2016**, *18*, 22914.

[53] K. Inamoto, M. Katsuno, T. Yoshino, Y. Arai, K. Hiroya, T. Sakamoto, "Synthesis of 3-substituted indazoles and benzoisoxazoles via Pd-catalyzed cyclization reactions: application to the synthesis of nigellicine" *Tetrahedron* **2007**, *63,* 2695.

[54] M. Taniguchi, J. S. Lindsey, D. F. Bocian, D. Holten, "Comprehensive review of photophysical parameters (ε, φ_f, τ_s) of tetraphenylporphyrin (H_2TPP) and zinc tetraphenylporphyrin (ZnTPP)– Critical benchmark molecules in photochemistry and photosynthesis" *J. Photochem. Photobiol. C Photochem. Rev*. **2001***, 146,* 59.

[55] Deposition numbers 2481135 (for **5aa**), 2481055 (for **5ab**) and 2481061 (for **5ac**) contain the supplementary crystallographic data for this paper. These data areprovided free of charge by the joint Cambridge Crystallographic Data Centre and Fachinformationszentrum Karlsruhe Access Structures service.

WILEY VCH